Int. J. Therm. Sci. (2000) 39, 490–497

S1290-0729(00)00204-0/FLA

Microscale boiling heat transfer under $0g$ and $1g$ conditions [1]

Johannes Straub *

Institut A for Thermodynamics, Technical University Munich, Boltzmannstrasse 15, 85748 Garching, Germany

(Received 31 October 1999, accepted 8 November 1999)

Abstract — Boiling heat transfer on a miniature heater has been studied in freon R11 under microgravity conditions during the Spacelab Mission IML-2 in 1994 and compared with measurements on earth. Several boiling modes have been observed depending on the liquid state, the subcooling of the liquid and the heat flux. The most important role in boiling heat transfer plays the surface tension, the wetting behaviour between the liquid and the solid surface of the heater, momentum of vapor formation, coalescence processes, and in subcooled liquids the thermocapillary driven convection. In the nucleate boiling region we could not observe a remarkable influence of the gravity on the heat transfer. In the film boiling and transition boiling region at moderate subcooling a maximum reduction of 50% of the heat transfer coefficient compared to the $1g$ data was found at this state. A single bubble with a 40 times larger diameter than the heater diameter of 0.26 mm, was attached at the top of the heater developing a strong thermocapillary jet flow. The observed heat flux densities and the values of the heat transfer coefficient are very high, even higher compared with wires. These experiments are basic studies to investigate the influence of the buoyancy force on the heat transfer and on the bubble dynamics, but additionally, they are simulations for the direct cooling of small electronic devices by pool boiling heat transfer, which becomes very important due to high thermal loads of modern electronic components even for the application in space vehicles. © 2000 Éditions scientifiques et médicales Elsevier SAS

boiling / miniature heater / thermocapillarity / buoyancy force / bubble dynamics / subcooled liquids / microgravity

1. INTRODUCTION

During the IML-2 Spacelab Mission of NASA in July 1994 (STS 65), we performed a pool boiling experiment in microgravity using a small thermistor with 0.26 mm in diameter simultaneously as the heating element and as a resistance thermometer [1, 2]. The experiment was accomplished in the BDPU (Bubble, Drop and Particle Unit), which is a Spacelab multi-user facility for fluid physics experiments in space operated by the European Space Agency, ESA. After the mission the measurements have been repeated on earth with the same facility and under the same conditions in order to get comparable values at $1g$.

The scientific objectives of these boiling experiments are listed as follows:

a) to study the mechanisms of boiling on a small spot heater of hemispherical geometry at microgravity and to compare the results with $1g$ reference data,

b) to observe the bubble growth, the bubble departure, the bubble size, in order to determine the influence of gravity on the bubble dynamics, as well as on the boiling process, and the heat transfer,

c) to investigate the heat transfer coefficient for a very small hemispherical microheater under $1g$ and microgravity, to find out the most important driving forces for the heat transfer if the buoyancy force is reduced to a negligible value ($a/g < 10^{-4}$),

d) to study the feasibility of using boiling heat transfer for the cooling of high powered microelectronic components immersed into a liquid, and its application in space and on earth [3–6].

2. EXPERIMENTAL HARDWARE

The BDPU is a multi-user facility designed and build by Alenia, Turin, Italy. The usability of this facility for

* jstraub@thermo-a.mw.tu-muenchen.de

[1] Based on a paper presented as a plenary talk at Eurotherm Seminar No. 57 “Microscale Heat Transfer”, Poitiers, France, July 8–10, 1998.

various experiments is ensured by special test containers which fulfill the specific experimental requirements. The facility itself provides the power supply for the test containers, the optical diagnostics with a background illumination, and a point diffraction interferometer arranged in two light paths perpendicular to each other. Each of them is recorded by a video camera and for the background illumination an extra 16 mm film camera is used. Furthermore, the BDPU provides the interface to the Spacelab and the Shuttle system for the video and the data link directly to the Operation Support Center at the NASA Marshall Space Flight Center (MSFC) in Huntsville, Alabama. There the principal investigators and their teams observed the experimental runs in real time video and all important experimental data have been directly available on computer screens. According to these observations the experiments are controlled by telecommanding from ground and new parameters can be adjusted. This system ensures that a maximum of scientific results is received.

The experimental test container was a precision engineered piece, designed and build by Ferrari, Modena, Italy, and Daimler–Benz Aerospace (Dornier), Friedrichshafen, Germany. All parts necessary for the accomodated experimental sequences are arranged in the narrow room of the container with the size of $45 \times 15 \times 30$ cm^3. The liquid cell itself is spherical with a diameter of 50 mm. It has four windows of sapphire with 40 mm diameter for the two observation directions perpendicular to each other. To change the pressure of the liquid cell and to compensate the vapor volume in order to keep the pressure constant during boiling, bellows are used with a counterpressure imposed by nitrogen. A small gas compressor supplied the pressure system and a small pressure vessel with the necessary compressed nitrogen. By that each experimental run could start at a pressure of about 6.5 bars, which was the upper limit due to safety regulations. Likewise of safety reasons our test container was build with a triple containment, to ensure that, in case of a leakage, no gas of the experimental fluid, freon R11, evaporates into the Spacelab environment.

Two Peltier elements on the lateral walls of the fluid cell were used both for heating and cooling. The temperature of the fluid could be controlled within ± 0.05 K. The Peltier elements dissipated the heat to the avionics air duct through two heat pipes. As heater we used a thermistor with an outer diameter of 0.26 mm and with an inner, electrically heated bead of 0.16 mm in diameter. It was selected in respect to its resistance characteristics. The thermistor top is formed as a hemisphere on the end of a cylinder with the same diameter and coated by a lead glass layer of about 0.05 mm thickness. The inner bead of the heater was electrically controlled at constant temperature T_{i}. Thus the wall temperature T_{w} at the outer surface of the heater, is given by

$$T_{\mathrm{w}} = T_{\mathrm{i}} - Q R_{\lambda} \tag{1}$$

with Q the heat flux determined by the voltage and current, the heat loss through the lead wires is subtracted. R_{λ} is the thermal resistance through the glass coating calculated with the hemispherical and cylindrical part of the heater. The heating power Q adjusted itself according to the controlled temperature, the thermal resistance, and the heat transfer coefficient to the liquid. With eight additional thermistors directly placed around the heater the liquid temperature is monitored. All data were recorded with a measuring frequency of 1 Hz. Within this time after the heater is switched on steady state condition was reached, because the heater's capacity is very small.

3. EXPERIMENTAL PROCEDURE

The original experiment was designed to study the growth of vapor bubbles in a homogeneous supersaturated liquid [1]. After the successful performance of this experiment we received from the NASA Control Center additional time for a boiling experiment. In order to perform this by using the same hardware and software, we could only control the heater in a constant temperature mode, but not in constant power mode as usual. To make the best use of the valuable microgravity time, the following experimental sequence was executed.

The temperature of the liquid and the pressure (6.5 bar) were set to the desired values. During stirring the liquid in the test cell was heated up to the set temperature. After the stirrer was switched off, the movement of the liquid calmed down within less than 2 min. The heater temperature T_{i} was set to the desired fixed value, and the heater was switched on. To assure steady state conditions one boiling point was held for 30 s. Without changing the heater's set temperature the pressure was stepwise reduced from 6.5 bar to the saturation value. At each pressure step boiling was recorded for 30 s. At the liquid temperature of 30 °C the saturated state was reached within 12 pressure steps. At the other liquid temperatures the boiling experiments were always performed at the same pressures. As mentioned before, the power adjusted itself according to the heat transfer to the liquid. The same experimental sequence was performed for each of the liquid temperatures 30, 40, 50, 60 and 70 °C, and each of the heater temperatures of 200, 180, 160 and 150 °C. By

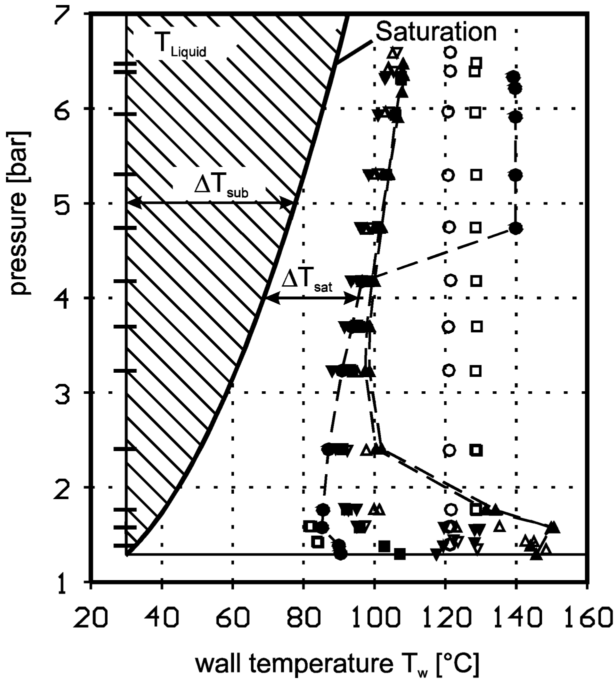

Figure 1. Boiling sequence at the liquid temperature of 30 °C in p, T- and p, q-plots. Full symbols microgravity, open symbols $1g$.

this way we obtained values in a wide range of subcooled (maximum 60 K at liquid temperature of 30 °C) and saturated liquid conditions. In the same sequence we repeated the experiments on ground after the mission.

4. BOILING SEQUENCE

In *figure 1* the results of an experimental sequence are shown in pressure versus temperature and heat flux plots at the liquid temperature of 30 °C and for four heater temperatures T_i. The calculated heater wall temperature T_w and the heat flux density q are monitored during the sequence and related to the liquid state. The curve in the p, T-plot is the saturation curve and the dashes perpendicular to the liquid isotherm at 30 °C indicate at which pressures measurements have been conducted. The full symbols represent the microgravity data, the open symbols the reference data under earth gravity. Interesting is that for the heater temperatures $T_i = 200$, 180, 160 °C, the heat flux density is increasing with decreasing subcooling, at about 30 K subcooling the heat flux has a maximum value and is moderately decreasing with a moderate increase of the wall temperature. However, at a subcooling of about 10 K the heat flux decreases strongly with a strong increase of the wall temperature. The evaluation of the data and the video recording show clearly that at these fluid states transition and film boiling occurs. The values of the heat flux oscillate with a periodical bubble departure and a strong thermocapillary flow develops. Important is to note that the reference data at earth gravity show the same behavior, however, with a comparable higher heat flux at the same subcooling. At saturation state the values of μg and $1g$ nearly coincide.

At the heater temperature of 150 °C nucleation occurs between the pressure step from 4.7 to 4.2 bar. The wall temperature was constant at 140 °C and decreased at nucleation to 94 °C (saturation temperature is 70.2 °C), respectively the heat flux increased from 90 to 560 kW·m^{-2}, while at $1g$ conditions no nucleation occurred all the way down to the saturated state, the wall temperature was constant with 121 °C, at a constant heat flux of 256 kW·m^{-2}. At the heater temperature of 160 °C in microgravity boiling sets in immediately, while at $1g$ nucleation occurs between the pressures 1.8 to 1.6 bar with a decrease of the temperature from 129 to 81 °C, and an increase of the heat flux from 300 to 750 kW·m^{-2}.

This different nucleation behavior is caused by the different temperature field around the heater. In microgravity it is determined by heat conduction only and is reg-

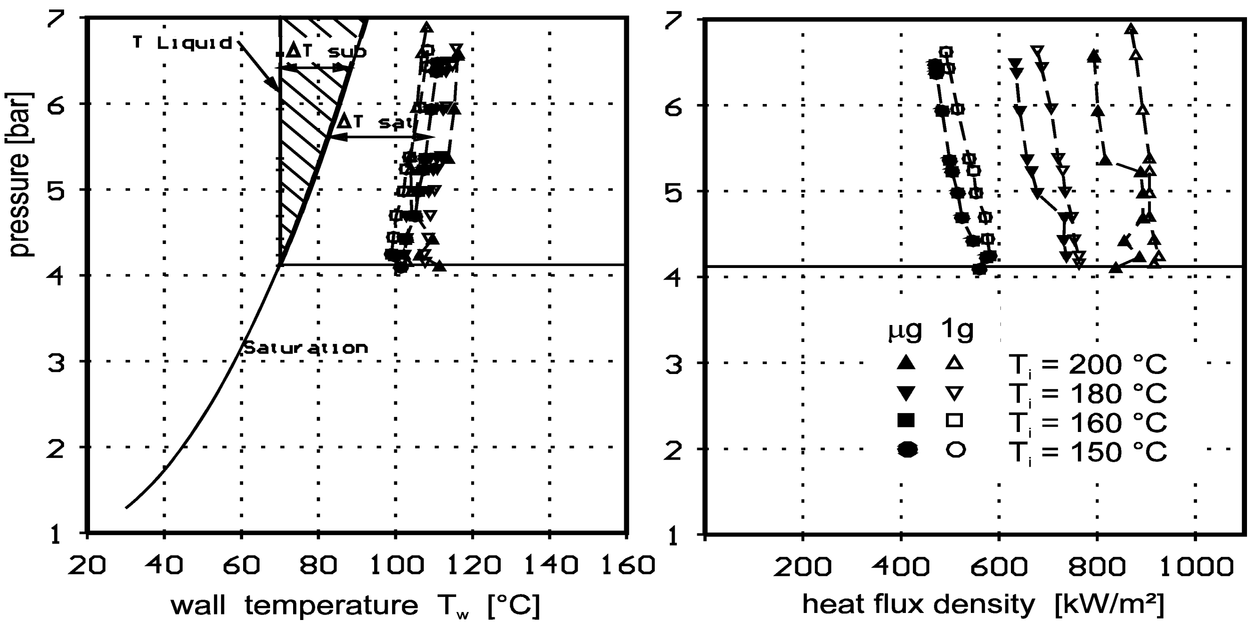

Figure 2. Boiling sequence at the liquid temperature of 70 °C in p, T- and p, q-plots.

ular around the heater. At $1g$ free convection determines the heat transfer and the temperature field in the liquid around the heater.

At the upper stagnation point the heat transfer to the liquid is less than at the lower stagnation point, therefore, the temperature at the upper stagnation point is higher, and nucleation will occur there first.

In *figure 2* the boiling sequence is shown for the liquid temperature of 70 °C. The behavior is quite different, with decreasing subcooling the heat flux is increasing down to saturation, and the temperature difference to saturation $\Delta T_{sat} = T_w - T_{sat}$ is slowly increasing.

5. BOILING MODES

During such an experimental sequence we observed various boiling modes, which are related to the course of the heater temperature, the heat flux and the associated heat transfer to the liquid.

5.1. Cavitation mode

At liquid temperatures of 30, 40 and 50 °C and at high subcooling down to $\Delta T_{sub} > 30$ K a “cavitation boiling mode” occurs. In spite of the high heat fluxes no bubbles are visible, but in the video recording of the interferometer a hot liquid plume (dark) is slowly moving with about 0.1–0.2 mm·s^{-1}. This observation is explained as detailed below. A thin boundary layer is superheated and nucleation occurs. After nucleation a very thin vapor film or small bubble is formed. Because of the great density difference between liquid and vapor it expands and pushes the liquid away. The vapor gets in contact with the subcooled liquid and condenses. This process with bubble growth and collapse repeats itself fast and pumps the hot liquid into the bulk, acting like a pump (bubble jet printer) with an estimated frequency of several kHz. At $1g$ this process is in principle the same, however, the hot liquid is transported by buoyancy convection with microconvection (the convection of the moving bubbles is meant).

5.2. Cavitation–thermocapillary flow–sparkling mode

At lower liquid subcooling between 30 and 10 K a mixed boiling mode occurs. The subcooling is no more sufficient to condense all the vapor immediately, small bubbles of the size of the thermistor become visible, they grow and condense, however, not immediately, a thermocapillary flow develops around them. With this flow subcooled liquid is transported to the interface of the bubbles, now the vapor can condense and the bubble

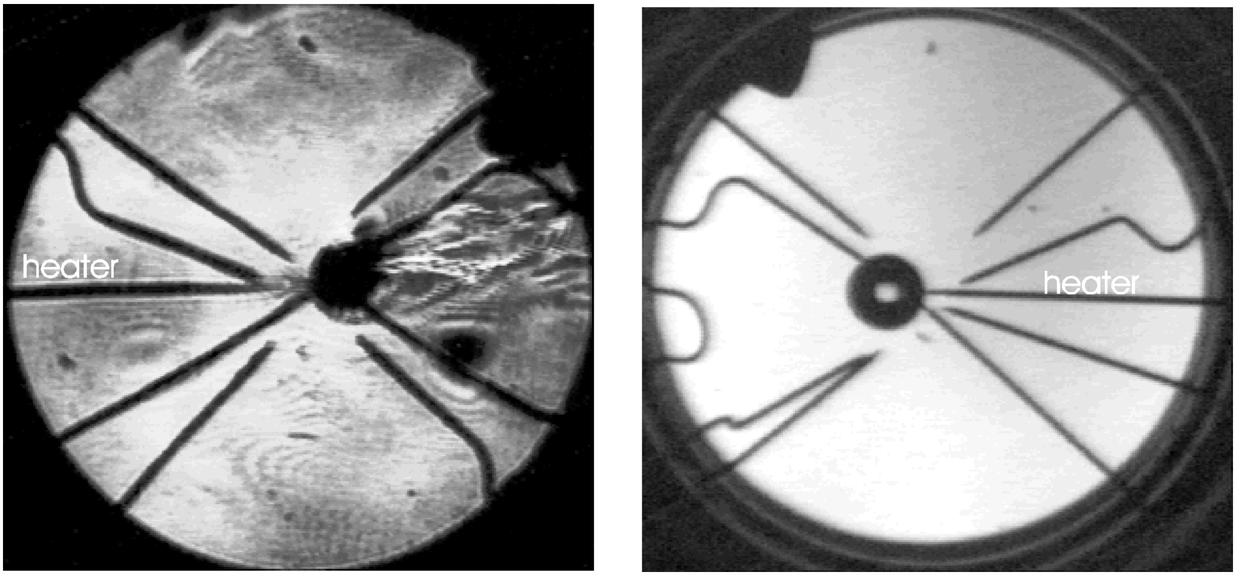

Figure 3. Thermocapillary jet mode. Left: point diffraction interferometer image. Right: background illumination image, turned 180°, the jet flow is not visible.

collapse. Thereby the heat flux is increasing a little. With the decrease of subcooling the bubbles on the heater increase to a size of 1–2 mm, with it the thermocapillary flow increases strongly, and this flow carries along small tiny bubbles like bubble sparkling. They condense in some distance from the heater.

5.3. Thermocapillary jet mode

At a subcooling of 10 K the bubbles which surround the heater form now one single bubble which does not collapse anymore. This bubble has first a size between 1 and 2 mm and is attached and centered stationary at the top of the heater. Around this bubble a strong thermocapillary convection develops, forming a turbulent trailing jet stream, like a turbulent "Karman Vortex Street". The reaction force of this stream presses the bubble at the heater. With the formation of the single bubble the heat flux is simultaneously reduced by 20–30 % and the wall temperature increases by 30 K. With the stepwise reduction of the pressure and, respectively, the subcooling, the bubble size increases stepwise too, to 5, 8 up to 10 mm, whereby the size at each step is kept constant and the bubble remains continuously at its top position, see *figure 3*.

With decreasing subcooling the heat flux is decreasing too, while the wall temperature is increasing. This indicates that at this jet mode a thin vapor film surrounds the heater itself. This vapor flows into the large bubble attached at the top of the heater and condenses at its inner surface, the thermocapillary convection carries the heat with the hot liquid away. For this transport the enlarged surface of the bubble, up to 2 000 times compared to the surface of the heater, is necessary, because with the decreasing subcooling the velocity of the thermocapillary flow and the driving temperature difference decreases. This surface area adjusted itself with the size of the bubble according to the heat flux and the subcooling.

At low subcooling, of about 2–3 K, the bubble grows up to 12 mm. Now the flow towards the bubble becomes equal to the flow away, the momentum forces become equal on both sides of the bubble in opposite directions, which results in an unstable situation. Slowly the bubble departs from the heater, sometimes it stands stationary at some distance from it, returns and departs again, always surrounded by a thermocapillary flow. After the departure a new bubble is growing and departing, the time sequence of this departure is about 20–30 s. With the departing frequency the heat flux is oscillating. At the departure the heat flux is reduced suddenly and increases slowly again with the growth of the bubble, in accordance with the larger surface more heat can be transported by thermocapillary convection.

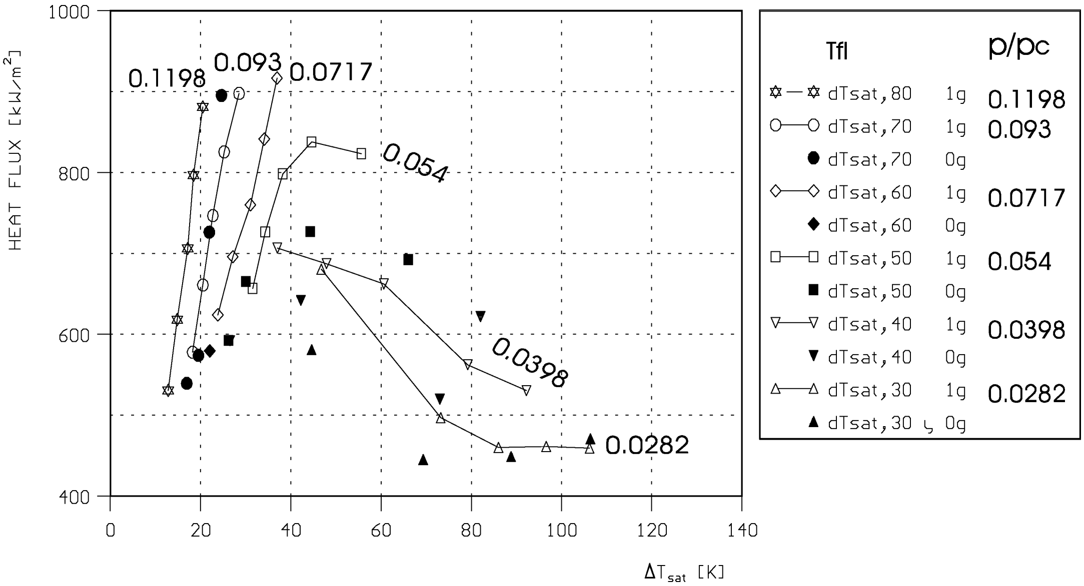

Figure 4. Boiling curves at saturation, full symbols μg, open symbols $1g$.

5.4. Saturated mode

At the saturation state no thermocapillary flow can be observed anymore. In the case of the lower liquid temperatures the bubbles depart in any direction with a size of 1–2 mm, and the heat flux oscillates with amplitudes of about 40 kW·m^{-2}. In accordance with the decreasing wall heater temperature and increasing heat flux this situation is typical of transition boiling on small heaters. It seems that the heater is covered partly with a vapor film, which periodically is contracted by the surface tension force to a single bubble and by that momentum the bubbles are pushed away and depart from the surface of the heater. At lower heat fluxes and at higher liquid temperature these effects are systematically reduced. At the liquid temperature of 70 °C normal nucleate boiling is observed, by the momentum of bubble formation the bubbles depart from the heater, see *figure 2*.

6. HEAT TRANSFER

Due to the limited space of this paper only the heat transfer for saturated liquid conditions is shown in *figure 4*. As usual, the heat flux is plotted versus the temperature difference ΔT_{sat}. At the liquid temperature of 50 °C the course from transition to nucleate boiling is observed with a maximum heat flux. The maximum heat flux in microgravity is about 15 % lower than at $1g$ conditions, but interesting is that it occurs at the same temperature ΔT_{sat}. According to the hydrodynamic theory the peak heat flux is related to the gravity, and at a reduced gravity of 10^{-4} this reduction should be larger. At liquid temperatures of 60 and 70 °C, normal nucleate boiling curves are achieved, with a strong increasing heat flux at a small increase of ΔT_{sat}, with a rate of about 50–60 kW·m^{-2} per 1 K. The $1g$ data plotted as open symbols are on the same curves. It is surprising that there is only a small difference in the nucleate boiling regime between microgravity and earth gravity data. This observation confirms our earlier statement [8, 9] that the influence of the gravity force on nucleate boiling is relatively small compared to most assumptions in existing correlations and it was the reason to establish the “microwedge model” for nucleate boiling [9, 10]. Remarkable are the high heat flux values which are about two times higher than on wires and ten times higher than on flat plates. In the film boiling and transition region the differences between μg and $1g$ are larger. At the liquid bulk temperature of 30 and 40 °C, transition boiling occurs with increasing heat flux at decreasing ΔT_{sat}, which corresponds to the observed bubble dynamics as described before. In microgravity the heat flux oscillates due to the single departing bubbles.

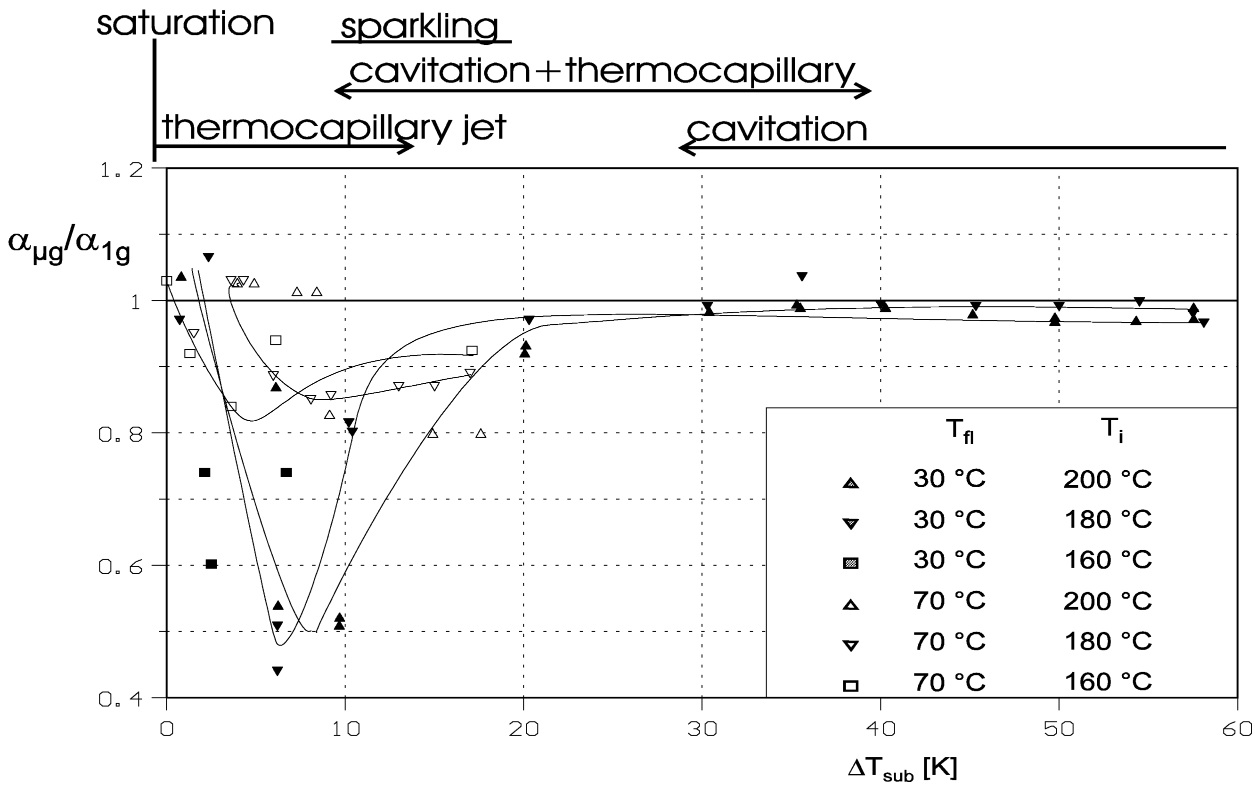

Figure 5. Gravity efficiency on heat transfer ratio $\alpha_{\mu g}/\alpha_{1g}$ versus subcooling, along constant liquid temperatures and various thermistor core temperatures T_i.

7. COMPARISON WITH THE DATA AT 1*g*

The best comparison of the heat transfer efficiency between the microgravity and earth gravity data can be made with the ratio of the heat transfer coefficients taken at the same liquid conditions. In *figure 5* this ratio is plotted versus the subcooled temperature for constant liquid temperatures as parameter during an experimental run.

At high subcooling in the "cavitation region" the heat transfer efficiency is only reduced by few percent. In the region described as "cavitation–thermocapillary flow–sparkling mode" between the subcooling of 30 to 10 K the efficiency drops down and is in the region of the "jet flow mode" lowest with about 50 % at the liquid temperature of 30 °C. With higher liquid temperatures and lower heat flux values (lower heater temperature) this efficiency coefficient is increasing and is around unity and sometimes even higher at saturation $\Delta T_{\text{sub}} = 0$ K.

8. CONCLUSIONS

These boiling experiments at saturated and subcooled liquid conditions performed at a very small hemispherical spot heater under microgravity and under earth gravity conditions lead to the following conclusions:

- Even for the small heater geometry we received in the nucleate boiling regime very high values of the heat flux at μg and at $1g$ up to 900 kW·m^{-2}. Compared, these values are two times higher than on wires, and ten times higher than on flat plates.
- A remarkable influence of the gravity on the overall heat transfer in the nucleate boiling region could not be observed, however, in the transition and film boiling region a reduction of up to 50 % is recorded.
- Furthermore, we must conclude that likewise the critical heat flux is not caused by hydrodynamic instability alone.
- We could observe several different modes of boiling in the subcooling state of the liquid, which are characterized

by different kinds of vapor formation and of bubble dynamics. These modes depend on the liquid state, on the subcooling, and on the heat flux, respectively on the surface temperature of the heater.

• These different regimes of bubble dynamics change immediately with the change of the subcooling state. The transition from one mode to the other is stimulated by thermo-hydrodynamic instabilities in the boundary layer of the heater, which needs a more detailed investigation.

• For the first time in the film boiling regime the thermocapillary jet mode was observed at moderate subcooling states. It is interesting to note that the high heat flux produced can be transported by this thermocapillary flow alone. However, this is only possible by the large surface area of the great bubble forming the trailing jet stream.

• Furthermore, it is important to note that even in microgravity, boiling is a very efficient process of heat transfer, and that it controls over a very wide range of heat dissipation its temperature itself by increasing or decreasing the heat flux. Therefore, the boiling process allows the application for direct cooling of high powered electronic microelements in all space systems. For such an application the liquid conditions can be optimized, as seen from our experimental results.

• The most important role for boiling heat transfer are: surface tension, wetting behaviour between the liquid and the heater material, coalescence processes, the momentum during bubble formation and in subcooled liquid states the thermocapillary flow [9, 10].

Acknowledgements

We would like to express our appreciation to all who made this research possible. Especially we are grateful to the Space Shuttle crew of STS 65, to NASA, especially to the Operation Support Center in Huntsville, AL, to ESA and ESA/ESTEC for providing the BDPU facility and the test container, to the German Space Agency DARA for financial support (contract 50WM9566). Furthermore, we thank all individuals and teams of the industrial companies Alenia, Laben, Ferrari and Dornier designing and building the facility and the test container, and for their support during the Mission.

REFERENCES

[1] Straub J., Winter J., Picker G., Zell M., Study of vapor bubble growth in a supersaturated liquid, in: Proc. of the National Heat Transfer Conference, Portland, Oregon, August 1995, HTD-Vol. 305, Vol. 3, ASME, 1995, pp. 29–37.

[2] Straub J., Winter J., Picker G., Zell M., Boiling on a miniature heater under microgravity—A simulation for cooling of electronic devices, in: Proc. of the National Heat Transfer Conference, Portland, Oregon, August 1995, HTD-Vol. 305, Vol. 3, ASME, 1995, pp. 61–69.

[3] Fushinobu K., Nagasaki T., Saitoh T., Ui A., Hijikata K., Boiling heat transfer characteristics from very small heaters on a substrate, in: Hewitt J. (Ed.), Heat Transfer 1994, Proc. of the 10th Int. Heat Conf., Brighton, U.K., Vol. 5, pp. 51–56.

[4] Baker E., Liquid immersion cooling of small electronic devices, Microelectronics and Reliability 12 (1973) 163–173.

[5] Bar-Cohen A., Fundamentals of nucleate pool boiling of highly-wetting dielectric liquids, in: Kakac S. (Ed.), ASI Proceedings, Cooling of Electronic Systems, Izmir, Turkey, 1993, pp. 415–455.

[6] Bergles A.E., Bar-Cohen A., Immersion cooling of digital computers, in: Kakac S. (Ed.), ASI Proceedings, Cooling of Electronic Systems, Izmir, Turkey, 1993, pp. 539–621.

[7] Forster H.K., Zuber N., Dynamics of vapor bubbles and boiling heat transfer, AIChE J. 1 (1955) 531–534.

[8] Straub J., Zell M., Vogel B., Pool boiling in a reduced gravity field, in: Hetsrony G. (Ed.), Proc. Ninth Int. Heat Transfer Conf., Jerusalem, Israel, 1990, Vol. 1, Hemisphere, New York, 1990, pp. 91–112.

[9] Straub J., The role of surface tension for two-phase heat and mass transfer in the absence of gravity, Experimental Thermal and Fluid Science 9 (1994) 253–273.

[10] Straub J., The microwedge model: A physical description of nucleate boiling without external forces, in: Materials and Fluids Under Low Gravity, Ninth Euro. Symp. on Gravity Dependent Phenomena in Physical Science, Berlin, 1995, pp. 351–358.